

# A multiparametric approach for rejuvenation of the Gaurikund geothermal spring system in the Northwest Himalayan region

Anurag KHANNA<sup>1</sup> , Debasish BAGCHI<sup>1</sup> ,  
Suresh KANNAUJIYA<sup>2,\*</sup> , Tandriila SARKAR<sup>3</sup> 

<sup>1</sup> Central Ground Water Board, Ministry of Jal Shakti, India

<sup>2</sup> Geosciences Department, Indian Institute of Remote Sensing,  
Indian Space Research Organisation, Dehradun, Uttarakhand, India

<sup>3</sup> Indian Institute of Technology (Indian School of Mines) Dhanbad, Jharkhand, India

**Abstract:** The Gaurikund town falls on the way of the famous trekking route to Kedar-nath that faced the wrath of the 2013 flood disaster. This fateful event severed more than 5000 casualties, demolished several infrastructures, and shifted the course of Gaurikund spring from its original position. Nevertheless, the Gaurikund geothermal spring system located in the Himalayan Geothermal Belt of the Garhwal region is preeminent for religious beliefs, balneotherapeutic values and a gateway to delve within the geothermal and hydrological characteristics of the area. In this perspective, restoration of Gaurikund geothermal spring system becomes a necessity. A multiparametric approach comprising geospatial, geology, hydrochemistry and geophysics has been used to study and justify these aspects at Gaurikund. The geological studies infer that the geothermal spring gets recharged by the steep, southerly dipping joints in granite gneiss. Subsequently, the deep percolated water heats up due to the high geothermal gradient and then emerge along the Vaikrita Thrust and its sympathetic minor fault-thrust system by advection. Moreover, four spring outlets are inventoried, with discharge varying from 7.46 to 95.54 L/min. The normal emissivity model uses the pre and post-disaster satellite data and generates maximum kinetic temperature images, showing a positive correlation between land surface temperature and spring discharge. Two-dimensional Electrical Resistivity Tomography (Schlumberger, Wenner and Gradient configurations) survey revealed two low resistivity zones proximal to the geothermal spring on the right bank of the Mandakini river. The engineering interventions carried out by bank protection and construction of small gully plugs in the catchment area is recommended along Gaurikund-Sonprayag section on the right bank of Mandakini river.

**Key words:** Himalayan Geothermal Belt, Geothermal spring, Electrical Resistivity Tomography, Normal Emissivity Model, Riverbank protection

\*corresponding author, e-mail: skannaujiya@gmail.com

## 1. Introduction

Spring systems in Indian Himalaya are characterized by distinct geotectonics, geomorphologic and hydrologic attributes. The rugged and surreal Himalayan range holds reins of the complex hydrological processes of springs and drives them through distinct geology, tectonics, landforms, and geomorphology (*Valdiya and Bartaya, 1991; Rawat, 2013, 2014*). About 15% of the Indian population relies on spring water, thus characterizing mountain ranges like Himalaya, Aravallis, Western & Eastern Ghats as springscapes. Himalaya has always been considered the largest springscape in the country, and hereby, it is significant to restore these valuable resources and maintain water security. But such allure is facing the wrath of anthropogenic activities and degrading geodiversity, disturbing the hydrological balance continually (*Rawat et al., 2012a,b; Bisht and Tiwari, 1996; Haigh et al., 1989; Hundecha and Bárdossy, 2004*). The propagation of groundwater flowing from within subsurface along the trails of planes with varying hydraulic conductivity into any water or land source is defined as Springs (*Schwartz and Zhang, 2003; Kresic and Stevanovic, 2010*). The natural springs provide for irrigation and drinking, and the source of such springs are generally unconfined aquifers. Subsequently, when rainfall pattern or infiltration rate varies, and spring discharge also varies as a consequence. Moreover, geothermal springs are a definitive source of inexpensive geothermal energy that can be incorporated in studies like climate and CO<sub>2</sub> emanations. For years the mountain livelihood has been devotedly dependent on spring water for their domestic and irrigation activities. So, rejuvenating spring is imperative for sustainable progress in these communities (*Bagchi et al., 2021*).

Recently, the rate of groundwater extraction has increased to quench each and every need of the civilization. In return, it has started showing severe consequences like land subsidence, parched wells and exhaustion of springs (*Sarkar et al., 2020, Karunakalage et al., 2021; Sarkar et al., 2022*). Therefore, the spring system of Himalaya helps restore rivers like Ganga, Narmada, Kaveri, Krishna, Godavari, and several other minor rivers (*NITI Aayog, 2018*).

The Himalayan Geothermal Belt (HGB) spans from Northwest (Ladakh) to Northeast (Assam) of India is characterized by numerous hot springs and

is considered as one of the highest heat flowing regions with  $> 200$  °C/km thermal gradient (*Shanker et al., 1991; Oldham, 1883; Chandrasekharam, 2010*). In HGB, water gets heated up within 1–2 km depth, sufficient for hot springs formation under appropriate hydrogeological conditions (*Rai et al., 2013*). Gaurikund geothermal spring is situated on the hanging wall of Vaikrita Thrust and is categorized as a fault spring (*Waring et al., 1965*). This geothermal spring is attributed to shallow crustal melting along subduction zone (*Hochstein and Regenauer-Lieb, 1998; Rai et al., 2013*), high radioactivity of leucogranite and gneisses (*Chandrasekhar and Chandrasekharam, 2007*) and high temperature because it lies within HGB having heat flow  $> 100$  mW/m<sup>2</sup>. In addition to that, Gaurikund lies in close vicinity to Vaikrita Thrust (MCT-I), which has a high thermal gradient and also, the rock water interaction significantly influences the spring (Fig. 1a & b).

The heat discharged from thermal fluids along the HGB gets concentrated as heat bands of 30–50 km wide and are segments of major, concentric slip lines caused by plastic deformation of the ductile crust within the Asian plate resulting from plate collision mostly in the Tibet region. These heat bands are associated with at least 600 geothermal systems in both Himalaya and Trans Himalayan region, including the Tibetan plateau (*Hochstein and Regenauer-Lieb, 1998*). A model explained by *Rai et al. (2013)* infers that meteoric water is the primary hot spring in MCT due to metamorphic CO<sub>2</sub> degassing through geothermal springs in Garhwal Himalaya. The CO<sub>2</sub> degassing occurs closer to hot springs, and it plays an essential role in its consumption by chemical weathering of silicate rocks.

In the MCT zone, it has been observed that most of the geothermal springs are located on the hanging wall side of the main thrust or its sympathetic faults. The north-south oriented lineament (third set of lineament) facilitated the emergence of hot water mainly along the Mandakini river valley through deep-seated extensional joints with relatively high fracture aperture. Therefore, the geothermal spring largely depends on the recharge scenario in the northern part of Gaurikund along the Mandakini valley. In the recharge area, precipitation is through snow and rainfall, and any change in the climatic conditions would alter the recharge condition of hot springs in the vicinity of Vaikrita Thrust or MCT-I.

Overall, all low and intermediate temperature systems derive heat from the hot, brittle upper crust through advective sweeps of infiltrated meteoric

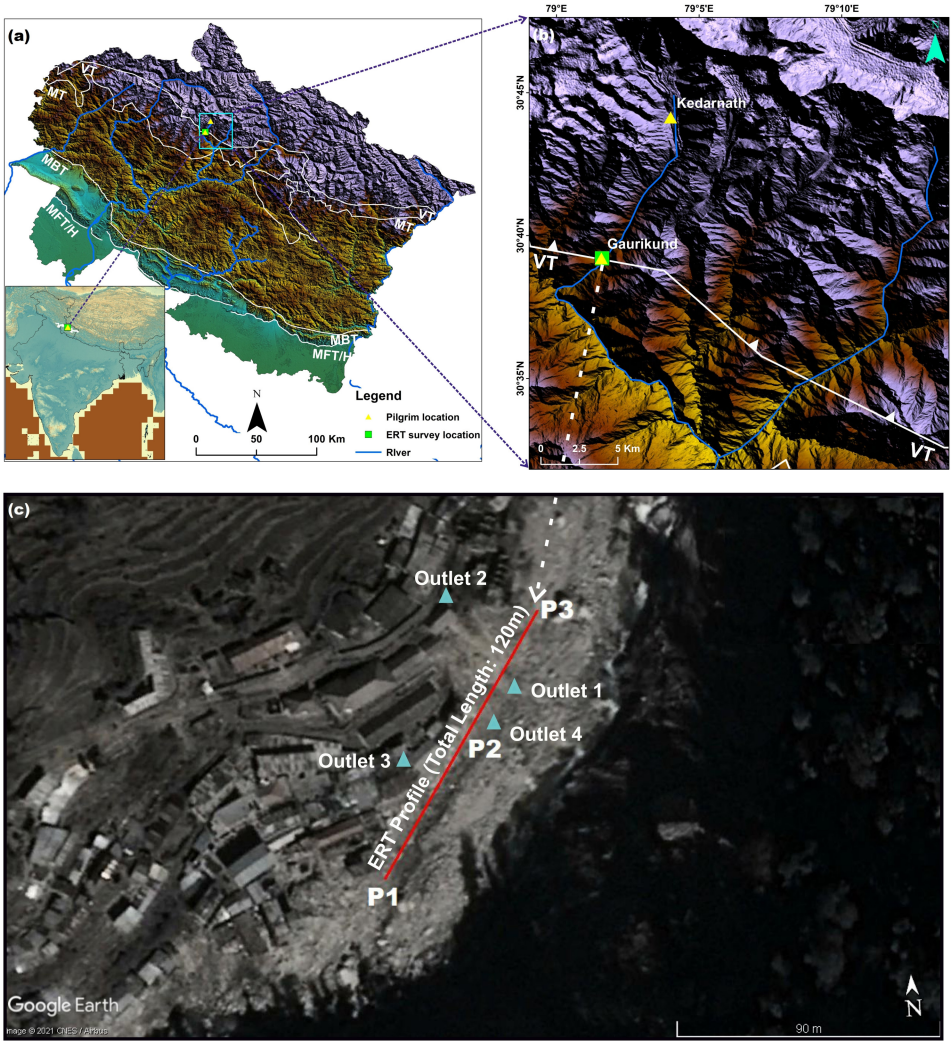


Fig. 1. (a) Study area showing the ERT locations and the pilgrim locations, the square with blue outline is enlarged in (b) featuring the location of Gaurikund (where ERT survey was carried out) along thrust system and the location of Kedarnath, a well-known pilgrimage along the rivers flowing in that area. (c) The ERT locations are magnified showing three different points P1, P2 and P3 having strike SSW-NNE and length of 120 m. Note the cyan blue colour triangles marks the position of four Outlets along the ERT profile.

water. High standing, cooling granitic plutons are probably the heat sources for a few systems with temperatures as high as 300 °C at a 1.5 km depth, e.g., Yangbajing in Tibet (*Hochstein and Regenauer-Lieb, 1998*). Similar granitic plutons and granitoid are present in the Indian side of the Himalayan Geothermal Belt, probably contributing to the high temperature of the Gaurikund spring through construction of RCC walls on both the left and right banks of Mandakini river along with area specific measures to arrest river bank flow.

In a similar observation in Nepal Himalaya, *Derry et al. (2009)* have summarized that most Himalayan hot springs are found along large incised valleys, in zones of steep river reaches and rapid fluvial downcutting. Most are located within or near the MCT zone and are associated with strong gradients in range-front topography and river profiles.

During 15–17th June 2013, Mandakini valley and many parts of Uttarakhand received unusual high precipitation of 300–400 mm accompanied with high snowmelt runoff in Higher Himalaya and led to unprecedented flooding, bank erosion, landslide/landslide lake outburst flood (LLOFs) and glacier Lake outburst Flood (GLOF) in valleys and downstream areas (*Petley, 2013; Dobhal et al., 2013; Rautela, 2013; Champati ray et al., 2016*). It was a widespread event that affected approximately 30,000 km<sup>2</sup> in Himachal Pradesh and all hill districts of Uttarakhand. As the time coincided with tourist/pilgrimage season, the total death toll was over 5,000, and most of the victims were classified as missing as per Indian law. Precipitation data obtained from Tropical Rainfall Measuring Mission shows an enormous rise of 346% in the rainfall of June compared to the previous five years average monthly rainfall of June (*Dubey et al., 2013, Uniyal, 2013; Allen et al., 2016*). The only operational rain gauge located in the upper slope region of Kedarnath had shown precipitation of 325 mm during the past 24 hours measured at 5.00 PM on 16th June (*Dobhal et al., 2013*). There were precisely two catastrophic events; the first occurred on the evening of 16th June, which was attributed to mainly landslides and LLOFs that destroyed some parts of Kedarnath, Rambara and Gaurikund. It was followed by GLOF on the 17th morning, which wiped out large portions of Kedarnath and downstream areas up to 120 km, affecting localities proportionate to their distance from the source region (*Rana et al., 2013*).

This research aims to understand the aftermath of the Kedarnath disaster on the Gaurikund geothermal spring system by integrated geospatial and geophysical techniques. Moreover, it also ponders the mitigation plan through construction of RCC walls on both the left and right banks of Mandakini river along with area specific measures to arrest river bank flow and future catastrophes.

## 2. Study Area

### 2.1. Geology of the area

The geology of the area comprises the Central Crystalline Group of MCT (a complex of metamorphic and granitic rocks), exposed along Gaurikund-Kedarnath foot track both upstream & downstream, and consists of two major litho-tectonic units demarcated by Vaikrita Thrust or MCT-I (*Valdiya et al., 1999; Kumar, 2005, Kannaujia et al., 2022*). The upper unit comprises grey garnetiferous gneiss (extremely foliated and weathered), schist, quartzite and migmatite (*Rautela et al., 2014*). And the general strike of the country rocks varies from  $N40^{\circ}E-S40^{\circ}W$  to  $N55^{\circ}E-S55^{\circ}W$  with a variable dip of  $38^{\circ}$  to  $51^{\circ}$  towards NW (Fig. 3a & b).

### 2.2. Regional and structural settings of the area

Three prominent joint systems (Fig. 9a) are conspicuous along the river section a) a prominent set defined by bedding joint or schistosity plane dipping N–NNE–NW at  $30-45^{\circ}$ , b) a steep joint set dipping S–SSW at  $55-65^{\circ}$  and c) a third major joint set across the earlier two sets, dipping very steeply ( $>75^{\circ}$ ) and oriented N–S to NNE–SSW, along which Mandakini river flows (Fig. 3b). On the downstream side of Gaurikund, a relatively gentle slope and the wide valley is developed compared to the upstream section of Mandakini river due to the intersection of three sets of joints and fault systems. The comprehensive meandering valley features of the Mandakini river is well perceived from the Corona satellite image of 1973 (Fig. 2). Also, the abrupt widening of Mandakini valley to the South of Gaurikund is geomorphic evidence indicating that the area is lying in proximity to a tectonic contact (*Rautela et al., 2014*).

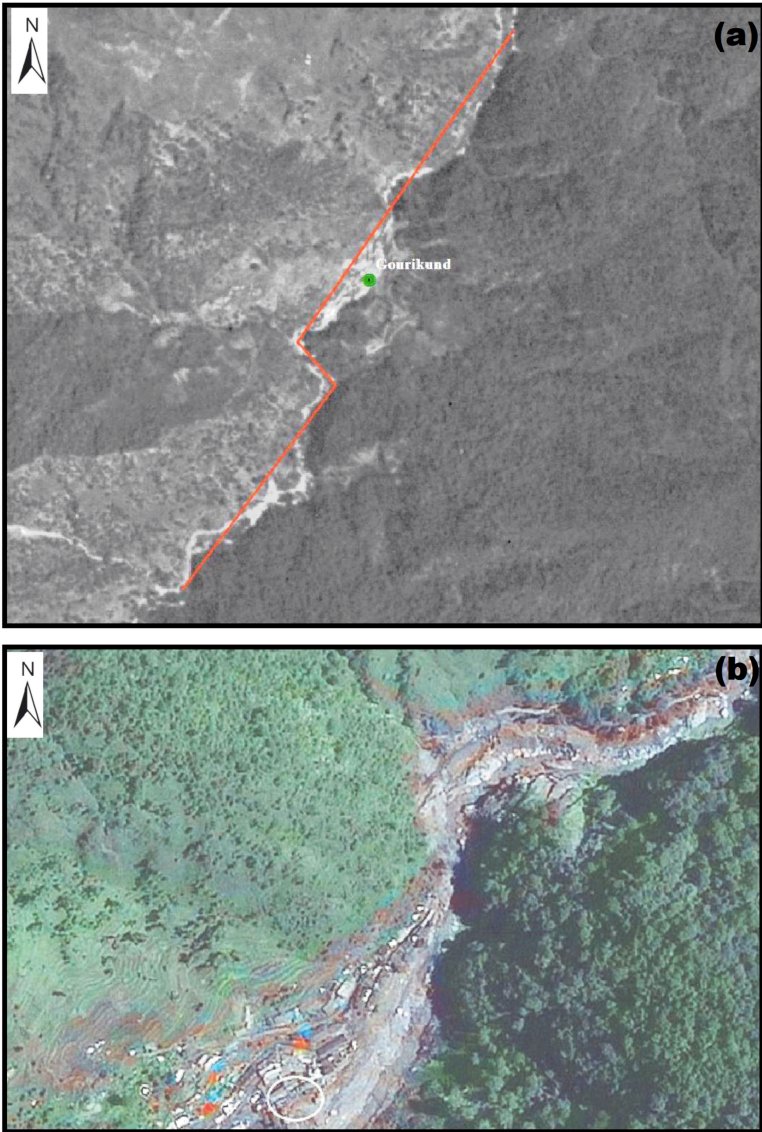


Fig. 2. (a) Offset by the major lineament (along which Mandakini river flows) due to thrust near Gaurikund (source: corona image, 24-11-1973). (b) Satellite image of Gaurikund and upstream section of Mandakini river (study area shown in white circle – data source: merged Cartosat-2 and LISS-IV in normal colour composite).

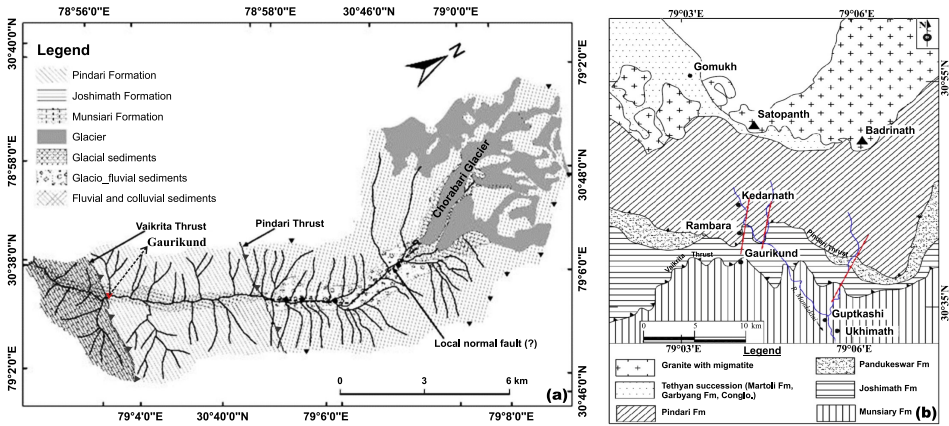


Fig. 3. (a) The regional geological map of Gaurikund and its surrounding areas (modified after *Dobhal et al., 2013*). (b) The regional structural map of the area, featuring in and around Gaurikund (modified after *Dobhal et al., 2013*).

### 3. Data and Methods

#### 3.1. Hydrogeological investigations

Both groundwater and rainfall are responsible for a spring recharge and accordingly characterize the Himalayan spring system. So, it is imperative to carry out the hydrogeological study to restrict the presence of groundwater within a placid geological setting. In this study, the authors have attempted to locate the present position of the Gaurikund geothermal spring, which had shifted from its original course after the Kedarnath 2013 disaster (Fig. 4). The hydrogeological study is carried out adjacent to the previous location of Gaurikund and the nearby temple situated on the right bank of the Mandakini river. It is inferred that the geothermal spring outlet got buried underneath huge boulders and debris generated by landslides and flash floods in the Mandakini river during the disaster. Rock outcrops composed of banded-streaky gneiss and porphyritic granite (intricately folded & deformed felsic bands) have been identified about 10 m north of the damaged and buried spring.

Consequently, four outlets of the previous geothermal springs (before the 2013 disaster) were identified by handheld GPS & in situ measurements



Fig. 4. (a) The red-coloured circle shows the Gaurikund location post devastation scenario from Kedarnath disaster. (b) The red arrows indicate Peak Flood Level of Mandakini river at Gaurikund during the occurrence of disaster. (c) Big boulders strewn near Tapt Kund, RCC retaining wall in the background.

and labelled as Outlet 1 to Outlet 4. An RCC retaining wall has been constructed on the posterior side of these major outlets (Fig. 4c). Due to the construction of this retaining wall and accumulation of debris, the geothermal spring has concealed itself under the debris cover and oozes out at different convenient locations (Fig. 5). These four outlets were further characterized in terms of the spring discharge, water and atmospheric temperature at varying elevation/altitude (Table 1).

Table 1. Location and other details of spring outlets at Gaurikund.

Point No.	Location	Altitude (m)	Discharge (L/min)	Temp. (°C)	
				Water	Air
1	Located ~ 10 m north of ladies bathing room, about 15 m from river course on the right bank of Mandakini river 30.6539°N, 79.0278°E	1972	9.00	58.0	20.0
2	Located near the base of RCC retaining wall, ~ 25 m west of river course, main source of geothermal spring with three sub-outlets 30.6542°N, 79.0275°E	1972	95.54	43.0	20.0
3	Located ~ 8 m downslope of Gauri Mata mandir, natural outlet ~ 5 m from the base of RCC retaining wall, ~ 20 m west of river course, on the right bank of Mandakini river 30.6536°N, 79.0272°E	1983	7.46	35.0	20.5
4	Located ~ 3 m south of ladies bathing room, ~ 20 m west of river course, on the right bank of Mandakini river 30.6538°N, 79.0277°E	1966	N/A	45.0	20.0

### 3.2. Hydrochemical investigation

Electrical Conductivity (EC) and spring water pH were measured in situ using HM Digital waterproof, portable EC, and pH meter during the ground survey. Three water samples collected from Outlets 1, 2 and 3 (Fig. 5) were

analyzed at Central Ground Water Board, Chandigarh (NABL Accredited Lab). The results of the chemical analysis are given in Table 2.

Table 2. Chemical analysis of water samples collected from hot spring, Gaurikund.

Sample No.	pH	EC ( $\mu\text{S}/\text{cm}$ )		Concentration (mg/L)						
		Field	Lab	$\text{NO}_3$	F	Cl	Ca	Mg	Na	K
<b>Gaurikund-Outlet-1</b>	6.40 (at 58 °C)	1300	1185	BDL	1.78	31	184	17	59	16
<b>Gaurikund-Outlet-2</b>	6.41 (at 43 °C)	1200	895	0.20	1.35	24	139	16	45	14
<b>Gaurikund-Outlet-3</b>	6.39 (at 35 °C)	400	394	0.72	0.4	10	55	10	14	7

BDL: Below Detection Limit



Fig. 5. Field photographs of primary outlets of Gaurikund geothermal spring (clockwise from top left: Outlet 1, Outlet 2, Outlet 3 and Outlet 4 having very feeble discharge not measurable during field survey).

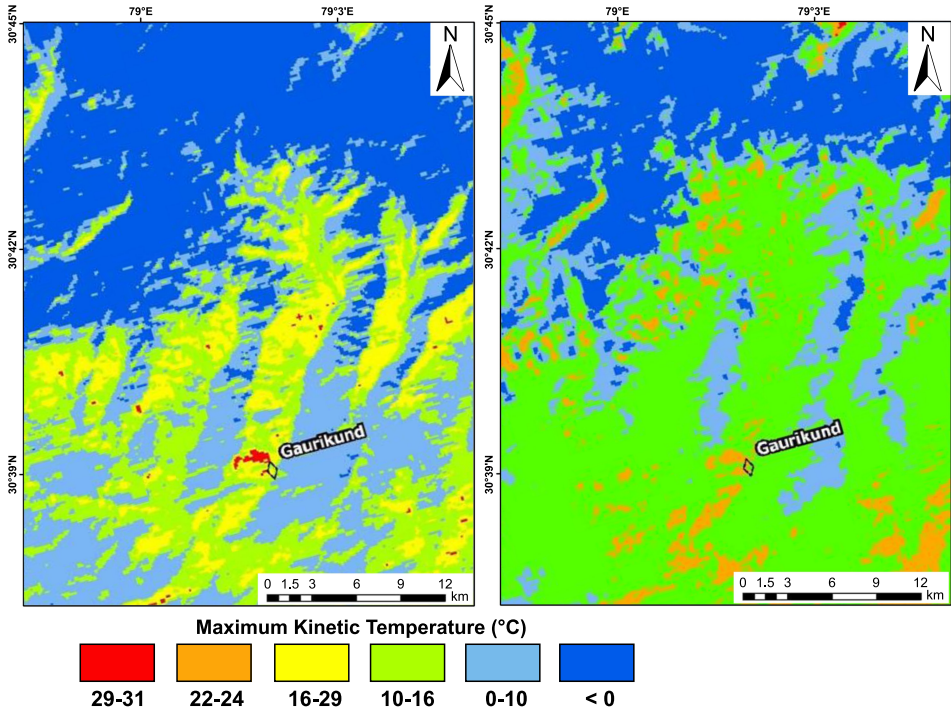


Fig. 6. (a) Maximum kinetic temperature image of Gaurikund and surrounding area before 2013 Kedarnath Disaster and the highest temperature seen at Gaurikund (data source: ASTER TIR image dated 12-9-2012). (b) Maximum kinetic temperature image of Gaurikund and surrounding area and the highest temperature zone (in red) is absent near Gaurikund post-2013 Kedarnath Disaster (data source: ASTER TIR image dated 03-11-2014).

### 3.3. Geospatial approach using the ASTER Thermal Infrared Imaging

ASTER Thermal Infrared (TIR) data sets were processed to detect thermal anomalies in Gaurikund area. The land surface temperature (LST) map was generated using ASTER TIR data acquired on 22.9.2012 (pre-disaster) and 3.11.2014 (post-disaster). The maximum kinetic temperature image for September 2012 was generated from multispectral data of ASTER TIR sensor using the Normal Emissivity Model (NEM). The 2012 thermal data shows a high-temperature region ( $> 29^{\circ}\text{C}$ ) north of Gaurikund town, coinciding with the geothermal spring source (Fig. 6).

### 3.4. Geophysical study by using the Electrical Resistivity Tomography

The subsurface features have different resistivity values, which are easily perceived by electric current flow. ERT survey is an excellent geophysical tool for identifying the various subsurface structures by measuring the distinct resistivity value of each material (Telford *et al.*, 1990; Kannaujiya *et al.*, 2019, 2021; Singh *et al.*, 2021; Haque *et al.*, 2020; Velayudham *et al.*, 2021). The inversion and modelling techniques are applied to obtain the true resistivity of the subsurface. Apparent resistivity is estimated from the following equation (Eq. (1)) and gives a probable resistivity value:

$$\rho_a = k \frac{\Delta V}{I}, \quad \text{where } k = \frac{2\pi}{\left\{ \frac{1}{r_{AC}} - \frac{1}{r_{BC}} - \frac{1}{r_{AD}} + \frac{1}{r_{BD}} \right\}}, \quad (1)$$

[ $k$  is a geometric factor, AB denotes the current electrodes, and CD indicates the potential electrodes].

Therefore, in forward modelling, RES2DMOD is used for apparent resistivity estimation of pseudo section (Loke, 2012). It includes both finite elements along with finite difference, thereby characterizing the subsurface into several rectangular blocks with respective resistivity values (Sasaki, 1992). Before moving on to inversion, all noises or disturbances are eliminated to estimate a true resistivity image. For this, RES2DINV software has been used to convert the apparent resistivity into true resistivity, while the least square optimization technique is employed for the inversion modelling (Loke and Barker, 1996). In addition to it, any demarcations present in the subsurface as boundaries are also removed by blocky optimization and iterative technique (Wolke and Schwetlick; 1988; Loke, 2012):

$$(J^T J + \lambda E_R) \Delta q_k = J^T R_d i - E_R q_k, \quad (2)$$

$$E_R = \alpha_x C_x^T R_m C_x + \alpha_z C_z^T R_m C_z,$$

[ $C_x$  is horizontal roughness filter,  $C_z$  is vertical roughness filter,  $J$  is a Jacobian matrix of partial derivatives,  $J^T$  is the transpose of  $J$ ,  $\lambda$  is a Damping factor,  $q$  is a model change vector,  $i$  is data misfit vector,  $\alpha_x$  and  $\alpha_z$  are the relative weights given to the smoothness filters in  $x$  and  $z$  direction, respectively].

Two-dimensional Electrical Resistivity Tomography (ERT) was carried out on the right bank of Mandakini river in open land adjacent to the buried geothermal spring source and temple complex using ABEM Terrameter-LS Earth Resistivity Meter. Two dimensional (2-D) ERT survey was carried out along profile line (P1–P2–P3) of 120 m oriented in NNE–SSW direction as this was the longest and most feasible profile line available in the region (Figs. 1c, 2b, 7). The topographically corrected resistivity sections for Wenner, Schlumberger and Gradient configurations are shown in Figs. 8a, 8b and 8c, respectively. The figures show subsurface electrical resistivity distribution up to a depth of ~25 m from the ground surface.



Fig. 7. The ERT survey being carried out on the right bank of Mandakini river, Gau-rikund.

## 4. Results

### 4.1. Inferences from the hydrogeological investigation

The field data shows Outlet 1 has the highest temperature of 58 °C with a discharge of 9.0 L/min and is considered closer to the main source. Outlet

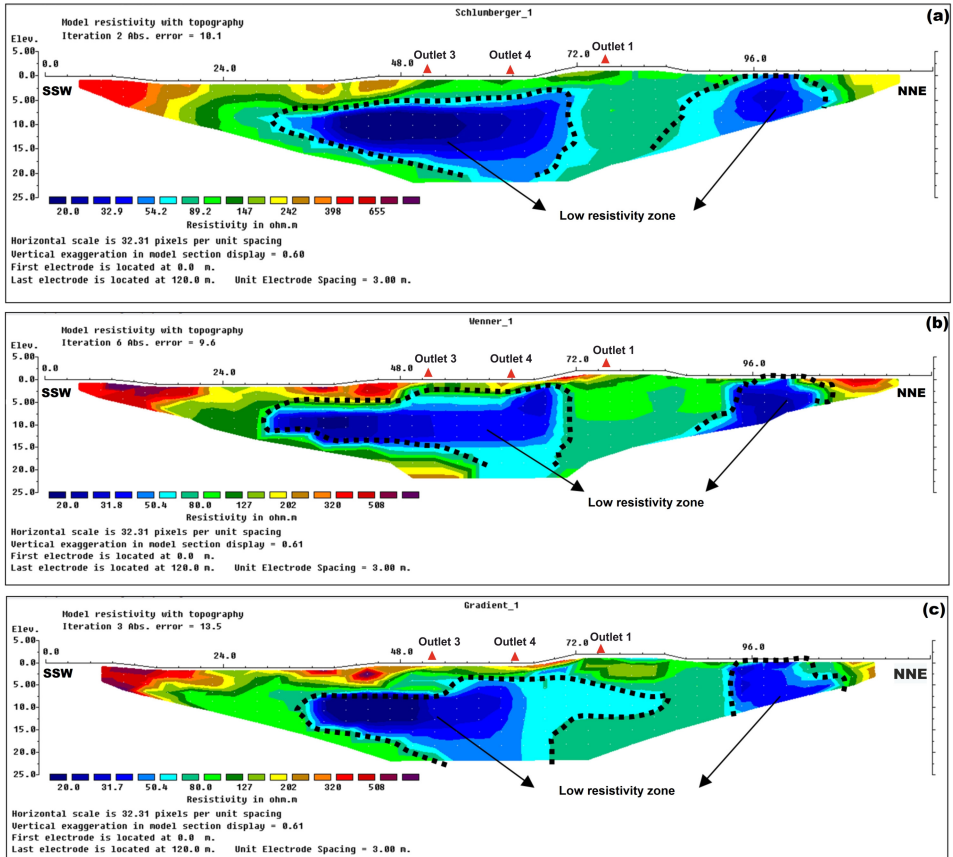


Fig. 8. (a) ERT section along the profile line P1–P2–P3 using the Schlumberger configuration (b) ERT section along the profile line P1–P2–P3 using the Wenner configuration (c) ERT section along the profile line P1–P2–P3 using the Gradient configuration. Note in all sections (a–c), the red triangles indicate position of Outlet 1 (~75 m), Outlet 2 (~62 m) and Outlet 3 (~53 m).

2, situated just down the slope of the RCC retaining wall and adjacent to Gaurikund temple, is the main source of the geothermal spring, showing the highest discharge of 95.54 L/min. It shows a relatively low temperature of 43 °C, mainly due to disturbances to the outlet due to debris cover and construction of the retaining wall. Outlet 3 shows the discharge of 7.46 L/min and temperature of 35 °C mainly due to intermixing of geothermal spring water either with cold groundwater or with the base flow of Mandakini river.

Mixing hot and cold spring water indicates hydraulic connectivity in the fractured rock aquifers locally developed in the high-grade granite gneiss, quartzite and migmatite of the Gaurikund Formation. Due to the feeble discharge and non-channelized flow of hot water at Outlet 4, the discharge measurement and sample collection were not possible. However, temperature, EC and pH were measured. A single natural outlet of hot spring, marked by characteristic reddish-brown outcrops at the base of the outlet, was observed on the left bank of the Mandakini river. Close field inspection of this outlet was not possible due to inaccessibility. Additionally, several minor discharges of geothermal spring water were observed further on the upstream side, marked by the reddish-brown colour of adjoining boulders on the river bed.

#### 4.2. Inferences from the hydrochemical investigation

The data shows that the geothermal spring water has relatively high EC at Outlet 1. High fluoride was reported from Outlet 1 and Outlet 2, which exceeds the acceptable limit of 1.0 mg/L for fluoride (*BIS, 2012*, IS:10500). Fluoride concentration at Outlet 1 even exceeded the permissible limit of 1.5 mg/L. High fluoride in spring water is attributed to fluoride bearing minerals in the granitoid around Gaurikund and Sonprayag. The EC, temperature, and fluoride concentration in groundwater at Outlet 3 are much less than Outlet 1 and Outlet 2, mainly due to mixing with the river's base flow. Concentrations of other constituents like nitrate, chloride, calcium and magnesium were within the acceptable limit (*BIS, 2012*). High sodium and potassium in spring water are attributed to rock-water interaction. Sodic and calcic plagioclase present in the granitoid act as the source of high sodium and potassium in the Gaurikund hot spring. Overall, it is observed that Outlet 1 is closer to the source compared to Outlet 2, which is partially disturbed due to debris cover and Outlet 3 is contaminated with the base flow of the river or local groundwater. Outlets 1 and 2 indicate intermediate temperature categories in comparison to major geothermal springs of the HGB. Overall, low pH indicates the source as meteoric water percolated down through fractures in the country rock, which reappears at the contact of major faults of the region.

### 4.3. Inferences from the geospatial approach

As the thermal image pre-dates the Kedarnath disaster of 2013, the anomaly related to the geothermal spring is compatible with the thermal signature, as shown in Fig. 6a. The figure shows a high kinetic temperature ( $24^{\circ}\text{C}$  to  $31^{\circ}\text{C}$ ) in the Gaurikund area, which correlates very well with the pristine condition of the hot spring. Thus, the maximum kinetic temperature map prepared using the TIR technique supports the ground-based hydrogeological survey, which measured in situ spatial distribution of land surface and water temperature in and around Gaurikund. The thermal image of the area after the 2013 Kedarnath disaster has been generated using ASTER TIR, and the maximum kinetic temperature image for post-monsoon (November 2014) using the NEM is shown in Fig. 6b. Interpretation of the image shows the absence of a high kinetic temperature zone in and around the geothermal spring source. The anomalous distribution of modelled temperature in and around Gaurikund is attributed to reduced spring discharge due to the burial of the original geothermal spring after the 2013 Kedarnath disaster. The substantial decrease in spring discharge is attributed to the diffused and non-channelized flow of geothermal spring in November 2014. The reduced spring flow measured during the post-monsoon ground survey validates the analysis of thermal image of the area using ASTER TIR data of November 2014.

### 4.4. Inferences from the geophysical approach

The ERT survey of Schlumberger, Wenner and Gradient configuration is carried out in Gaurikund by employing 40 electrodes, and respective three profiles are derived, trending in NNE–SSW direction (Figs. 1, 8). These profiles are topographically corrected, and Inverse modelling is used to estimate the true resistivity value. In each respective profile, the electrode spacing is 3 m. After running about 2 (Schlumberger), 6 (Wenner), 3 (Gradient) iterations, the ABS error achieved for each distinctive profile is 10.1, 9.6 and 13.5%, respectively. The low resistivity zones are indicated by dark blue patches (encircled in dotted black) that are seen in all the three profiles having resistivity values between  $\sim 20\text{--}50\ \Omega\text{m}$ . Such low resistivity zones indicate the path for the flow of water (*Metwaly and AlFouzan, 2013*).

Simultaneously, the high resistivity value zones are highlighted by green-yellow, red-orange colour in each profile and are quite sporadically present. Also, to infer a spatial idea about the locations of four Outlets on the ERT profile we have extrapolated from the ERT profile towards the locations of the Outlets. The results show that Outlet 1 and 4 are on the right side of the profile at an approximate distance of 75 m and 62 m respectively (indicated by red triangles as shown in Fig. 8). The Outlet 3 falls on left side of the profile at an approximate distance of 53 m (indicated by red triangles as shown in Fig. 8). It is also observed that Outlet 2 didn't fit within the extrapolation as it lies quite far away from the ERT profile and very close towards settlements (Fig. 1).

## 5. Discussions

### 5.1. The aftermath of the Kedarnath 2013 disaster

In the disaster of 2013, the major part of Gaurikund town, temple complex and geothermal spring source were severely damaged or buried under debris. As it is an essential geothermal spring of the region and has a lot of religious sentiments and balneotherapy values, there was widespread concern (including Green Tribunal intervention) and demand to revive the spring and restore the surroundings. Kedarnath is located at an elevation of 3553 m above sea level and is famous as a pilgrim town. But on 15–18 June 2013, the catastrophic flood doomed this pilgrimage city. The water level rose obstinately above the danger line both in Mandakini and other river systems. This tragedy hit the local infrastructure and the surroundings, thereby destroying several hydroelectrical projects. It is believed that topography or orography and human intervention were also responsible for such calamity. The significant impact of the disaster was due to landslides, bank erosion, and Chorabari Tal breaching on 16th and 17th June 2013 (Dobhal et al., 2013; Rautela, 2013; Martha et al., 2015; Champati ray et al., 2016). The devastating flood that destroyed Gaurikund spring and adjoining areas on the right bank of Mandakini River is primarily attributed to the narrowing of the river course slightly upstream of Gaurikund. During the fateful event, the left bank of Mandakini River (opposite slope of Gaurikund) experienced severe erosion and bank failure followed by a mas-

sive landslide (400 to 425 m long,  $\sim 85$  m wide), which partially blocked the river course (Dobhal *et al.*, 2013). As a result, the flow was diverted towards Gaurikund and subsequently destroyed and buried the geothermal spring source and bathing complex, part of the temple complex and surrounding areas, including an iron bridge. The river had severely affected areas up to 40 m from the right bank, where most structures were situated. The aftermath scenario of the devastation effect has been captured through the field photographs (Fig. 3a–c). The High Flood Level (HFL) of the Mandakini river during the disaster is shown in Fig. 3b, it is distant approximately 30 m from the original riverbed. In fact, in most of the upper reaches of the Mandakini river, the HFL (2013) was around 20–30 m from the riverbed, which resulted in a two to four times increase in river width in narrow valleys causing bank erosion and landslides.

## 5.2. A mitigation plan to restore and rehabilitate the Gaurikund geothermal spring

In order to restore the geothermal spring and minimize damage to life and property and control the erosion by the Mandakini river, it is suggested to implement riverbank protection, restoration and reconstruction of the geothermal spring outlet and a storage pond for socio-religious activities. During the 2013 disaster, the river developed avulsion towards the west, so bank protection is required to reclaim area keeping adequate waterway for passing excess flood water in future. To minimize future flood hazards and increase bank stability, Flood Protection Wall (FPW) needs to be constructed on both banks of the river, which covers an entire stretch ( $\sim 300$  m) of Mandakini starting from north of Gaurikund to the south of the iron bridge on Gaurikund-Sonprayag road. The western side (right bank of Mandakini river), where important outlets of hot spring, temple and human settlement are located, will get double protection from the envisaged structure and the existing retaining wall. Field investigations have shown that the flood water had reached approximately 30 m above the riverbed in 2013. Therefore, it is essential to make two tier flood protection wall for minimizing the damaging effect of future extreme events.

The geothermal spring water is currently un-channelized due to the construction of retaining walls and debris cover of the 2013 disaster. Therefore,

we propose that the spring sources flowing beneath the retaining wall be diverted into a new storage tank/bathing complex for religious activities. In order to reduce the loss of discharge from hot springs, it is also proposed to drill and provide horizontal perforated pipes to collect water in a large pond. A schematic diagram of the proposed FPW, renovated geothermal spring and bathing complex is shown in Fig. 9b. In this endeavour, it is also suggested to collect water from Outlets 1 and 2 together to the proposed pond, which will increase the flow and maintain the high temperature of the water. Outlet 3 being of lower temperature and contaminated with the base flow is not considered. However, attempts should be made in future to source other outlets of primary source in the near vicinity and channelize the flow to the proposed pond. The pre-requisites to determine the impact of spring rehabilitation at Gaurikund are measuring cumulative spring discharge and assessing the total volume of spring water available. Assessment and comparison with the dimensions of the pre-disaster pond (kund) suggest that the storage volume for rehabilitation of the spring is sufficient, considering an uninterrupted flow. The most immediate intervention would be to construct Flood Protection Walls on both banks of the Mandakini river and drill on the right bank adjacent to the temple complex. A series of gully plugs must be constructed along the seasonal streams (khudds and gads) that flows into the Mandakini river in the Gaurikund temple complex's upstream section. These gully plugs will arrest the monsoon runoff and help in water conservation, facilitating the shallow recharge, leading to deep percolation for rejuvenation of the hot spring source. Small gully plugs are suitable to arrest torrential monsoon flows in addition to water conservation during the non-monsoon period. Riverbank protection along the Gaurikund-Sonprayag section will be achievable by constructing a series of gully plugs (height 1.5–2.0 m, base width 2.0 to 3.0 m) and the Flood Protection Wall on the right bank of Mandakini. Monitoring of river flow (stage, discharge, silt content) and studying variation in cross-section of riverbed should be done at regular intervals to assess the changes in surface flow regime. Periodic monitoring of discharge and water quality will help evaluate the variation in the hydrological-hydrogeological regime of the Gaurikund area, which is a pre-requisite for implementing sustainable spring rehabilitation, disaster management and mitigation programmes. Recharge areas for the hot spring are located upstream of Gaurikund and in the

catchment of the Mandakini river. Thus, appropriate water conservation measures and monitoring of spring discharge and spring water chemistry are required at regular intervals.

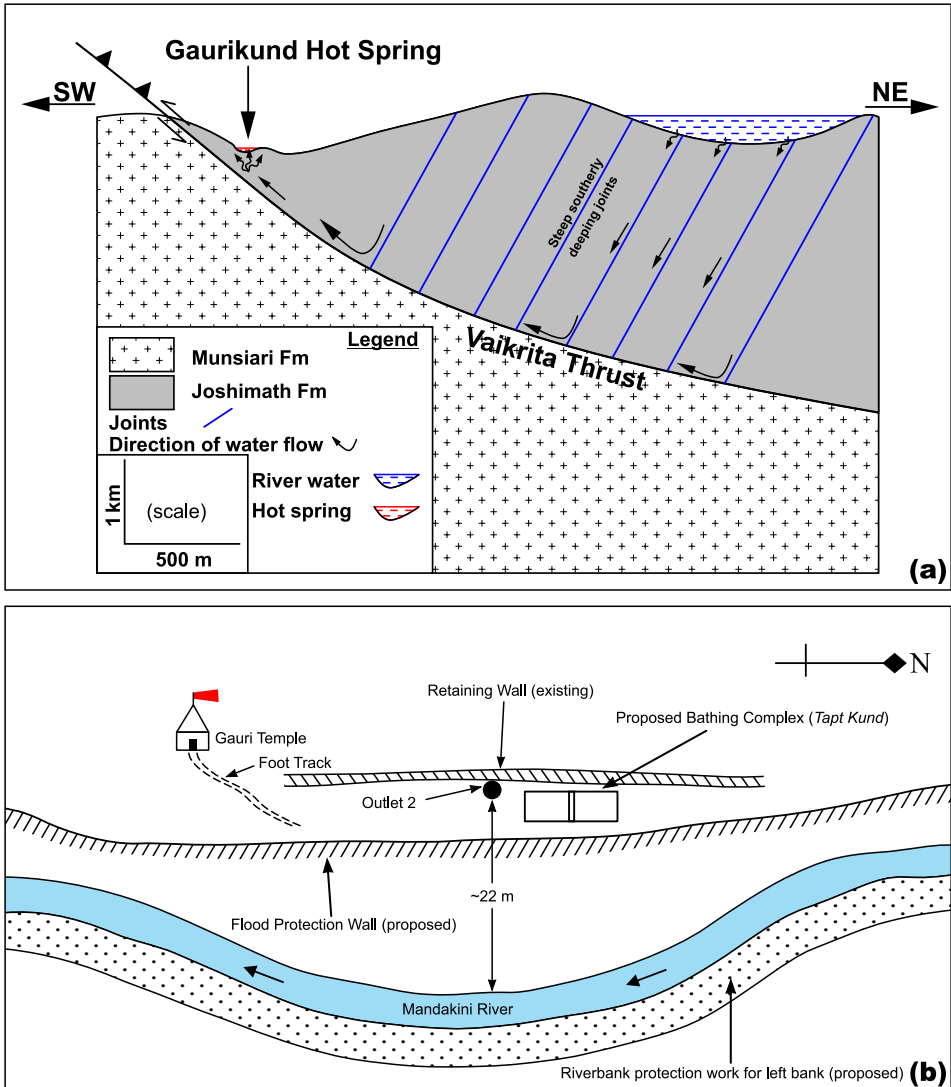


Fig. 9. (a) The pivotal thrust and joint system found in formation of hot spring at Gaurikund. (b) A Schematic representation of a rehabilitation plan for Gaurikund hot spring.

## 6. Conclusion

The geothermal sources of the Himalaya are significant due to religious and medicinal values and their geochemical signature of host rock and water interaction. Additionally, these play a vital role in the assessment of global climate due to degassing of CO<sub>2</sub>. A detailed study of hot springs in the Indian HGB region is lacking today, which calls for the preservation of such sites for future studies. The present study focuses on rejuvenating the geothermal spring at Gaurikund (Higher Himalaya), buried due to landslide and river-borne materials. Also, the Kedarnath disaster of 2013 has significantly affected terrain slope, riverbank of Mandakini and local hydrological regime around the Gaurikund geothermal spring. The hydrogeological setup of the area suggests that the recharge zone of Gaurikund spring is to the north of the town. The Mandakini river flowing in a valley marked by lineaments, joints and fractures, acts as the main conduit for recharge, followed by deep percolation and emergence along the fault-thrust system developed around Gaurikund. The channelized flow of hot spring water has been facilitated by faults/thrusts in the brittle part of the upper crust associated with the Vaikrita Thrust, a part of the Main Central Thrust system. Thermal remote sensing using Normal Emissivity Model has indicated an anomalous distribution of modelled temperature in and around Gaurikund. This is attributed to reduced spring discharge post-disaster due to the burial of the original geothermal spring source under the thick debris cover observed during the present study. The pre-requisites to determine the impact of spring rehabilitation at Gaurikund are measuring cumulative spring discharge and assessing the total volume of spring water available. Assessment and comparison with the dimensions of the pre-disaster pond (kund) suggest that the storage volume for rehabilitation of the spring is sufficient, considering an uninterrupted flow. The most immediate intervention would be to construct Flood Protection Walls on both banks of the Mandakini river and drill on the right bank adjacent to the temple complex. A series of gully plugs must be constructed along the seasonal streams (khudds and gads) that flows into the Mandakini river in the Gaurikund temple complex's upstream section. These gully plugs will arrest the monsoon runoff and help in water conservation, facilitating the shallow recharge, leading to deep percolation for rejuvenation of the hot

spring source. High fluoride in Gaurikund spring water is a potential health hazard that requires periodic assessment on temporal variability in fluoride and the possible balneotherapeutic value of the hot spring. The integrated geologic-hydrogeologic-chemical-geophysical-remote sensing-engineering approach to study Gaurikund geothermal spring can be replicated in the HGB, where spring restoration is necessary for sustaining people's livelihood.

**Acknowledgements.** This paper is dedicated to late Dr. P. K. Champati ray, Scientist-G and Group Head, Geosciences and Disaster Management Studies Group, Indian Institute of Remote Sensing, Dehradun, India for his indefatigable spirit in the pursuit of scientific excellence. Dr. ray was actively involved during preparation of this manuscript and did revise the full text twice before his untimely demise. He was instrumental in initiating geospatial studies in the Lesser and Central Himalaya in general, and in the characterization of Gaurikund geothermal spring in particular. Special thanks are to Dr. Dipankar Saha, Member (Retd.), Central Ground Water Board, Govt. of India for valuable inputs during finalization of this manuscript. The authors are thankful to the Chairman, Central Ground Water Board, Ministry of Jal Shakti, Govt. of India for giving encouragement during preparation of the paper. Special thanks are due to Dr. Prakash Chauhan, Director, Indian Institute of Remote Sensing (IIRS), India for providing full support to this study. The authors also express their gratitude to Dr. R. S. Chatterjee, IIRS, Dehradun, India for conceding the analysis on thermal data. The authors are thankful to Dr. Sashikant Singh, Mr. S. Bhatnagar and Mr. R. Annavarapu of Central Ground Water Board, Ministry of Jal Shakti, Govt. of India for rendering invaluable support during the geophysical survey. The authors are highly obliged towards Editor Prof. Dr. Roman Pašteka and the anonymous reviewer whose wonderful suggestion and comments have helped us in carving out a niche of our research work.

## References

- Allen S. K., Rastner P, Arora M., Huggel C., Stoffel M., 2016: Lake outburst and debris flow disaster at Kedarnath, June 2013: Hydrometeorological triggering and topographic predisposition. *Landslides*, **13**, 6, 1479–1491, doi: 10.1007/s10346-015-0584-3.
- Bagchi D., Kannaujiya S., Champati ray P. K., Taloor A. K., Sarkar T., 2021: A study on spring rejuvenation and springshed characterization in Mussoorie, Garhwal Himalaya using an integrated geospatial-geophysical approach. *Remote Sens. Appl. Soc. Environ.*, **23**, 100588, doi: 10.1016/j.rsase.2021.100588.
- Bisht B. S., Tiwari P. C., 1996: Land-use planning for sustainable resource development in Kumaon Lesser Himalaya—a study of the Gomti watershed. *Int. J. Sustain. Dev. World Ecol.*, **3**, 4, 23–34, doi: 10.1080/13504509609469932.
- BIS (Bureau of Indian Standard), 2012: IS:10500 Drinking Water – Specifications (2nd Revision), Manak Bhavan, New Delhi.

- Champati ray P. K., Chattoraj S. L., Bisht M. P. S., Kannaujiya S., Pandey K., Goswami A., 2016: Kedarnath disaster 2013: causes and consequences using remote sensing inputs. *Nat. Hazards*, **81**, 1, 227–243, doi: 10.1007/s11069-015-2076-0.
- Chandrasekhar V., Chandrasekharam D., 2007: Enhanced Geothermal Resources: Indian Scenario. *Trans. Geotherm. Resour. Counc.*, **31**, 271–274.
- Chandrasekharam D., 2010: Geothermal Energy Resources of India: Country Update, Proceeding of World Geothermal Congress, May 28 – June 10, 2010, Kyushu – Tohoku, Japan.
- Derry L. A., Evans M. J., Darling R., France-Lanord C., 2009: Hydrothermal heat flow near the Main Central Thrust, central Nepal Himalaya. *Earth Planet. Sci. Lett.*, **286**, 1-2, 101–109, doi: 10.1016/j.epsl.2009.06.036.
- Dobhal D. P., Gupta A. K., Mehta M., Khandelwal D. D., 2013: Kedarnath disaster: facts and plausible causes. *Curr. Sci.*, **105**, 2, 171–174.
- Dubey C. S., Shukla D. P., Ningreihon A. S., Usham A. L., 2013: Orographic control of the Kedarnath disaster. *Curr. Sci.*, **105**, 11, 1474–1476.
- Evans M. J., Derry L. A., France-Lanord C., 2008: Degassing of metamorphic carbon dioxide from the Nepal Himalaya. *Geochem. Geophys. Geosyst.*, **9**, 4, Q04021, doi: 10.1029/2007GC001796.
- Haigh M. J., Rawat J. S., Bisht H. S., 1989: Hydrological impact of deforestation in Central Himalaya. In: *Proceedings hydrology of mountainous areas, Czechoslovakia, IHP/UNESCO*, 425–426.
- Haque S., Kannaujiya S., Taloor A. K., Keshri D., Bhunia R. K., Champati ray P. K., Chauhan P., 2020: Identification of groundwater resource zone in the active tectonic region of Himalaya through earth observatory techniques. *Groundw. Sustain. Dev.*, **10**, 100337, doi: 10.1016/j.gsd.2020.100337.
- Hochstein M. P., Regenauer-Lieb K., 1998: Heat generation associated with collision of two plates: the Himalayan geothermal belt. *J. Volcanol. Geotherm. Res.*, **83**, 1-2, 75–92, doi: 10.1016/S0377-0273(98)00018-3.
- Hundecha Y., Bárdossy A., 2004: Modeling of the effect of land use changes on the runoff generation of a river basin through parameter regionalization of a watershed model. *J. Hydrol.*, **292**, 1-4, 281–295, doi: 10.1016/j.jhydro1.2004.01.002.
- Kannaujiya S., Chattoraj S. L., Jayalath D., Champati ray P. K., Bajaj K., Podali S., Bisht M. P. S., 2019: Integration of satellite remote sensing and geophysical techniques (electrical resistivity tomography and ground penetrating radar) for landslide characterization at Kunjethi (Kalimath), Garhwal Himalaya, India. *Nat. Hazards*, **97**, 3, 1191–1208, doi: 10.1007/s11069-019-03695-0.
- Kannaujiya S., Philip G., Champati ray P. K., Pal S. K., 2021: Integrated geophysical techniques for subsurface imaging of active deformation across the Himalayan Frontal Thrust in Singhauli, Kala Amb, India. *Quat. Int.*, **575–576**, 72–84, doi: 10.1016/j.quaint.2020.05.003.
- Kannaujiya S., Yadav R. K., Champati ray P. K., Sarkar T., Sharma G., Chauhan P., Pal S. K., Roy P. N. S., Gautam P. K., Taloor A. K., Yadav A., 2022: Unraveling seismic hazard by estimating prolonged crustal strain buildup in Kumaun-

- Garhwal, Northwest Himalaya using GPS measurements. *J. Asian Earth Sci.*, **223**, doi: 10.1016/j.jseaes.2021.104993.
- Karunakalage A., Sarkar T., Kannaujiya S., Chauhan P., Pranjali P., Taloor A. K., Kumar S., 2021: The appraisal of groundwater storage dwindling effect, by applying high resolution downscaling GRACE data in and around Mehsana district, Gujarat, India. *Groundwater for Sustainable Development*, **13**, 100559, doi: 10.1016/j.gsd.2021.100559.
- Kresic N., Stevanovic Z., 2010: *Groundwater Hydrology of Springs: Engineering, Theory, Management, and Sustainability*. Butterworth-Heinemann (Elsevier).
- Kumar G., 2005: *Geology of Uttar Pradesh and Uttaranchal*. Geological Society of India, Bangalore, 383 p.
- Loke M. H., 2012: *Tutorial: 2-D and 3-D Electrical Imaging Surveys*. Geotomo Software, Malaysia.
- Loke M. H., Barker R. D., 1996: Rapid Least-Squares Inversion of Apparent Resistivity Pseudosections by a Quasi-Newton Method. *Geophys. Prospect.*, **44**, 1, 131–152, doi: 10.1111/j.1365-2478.1996.tb00142.x.
- Martha T. R., Roy P., Govindharaj K. B., Kumar K. V., Diwakar P. G., Dadhwal V. K., 2015: Landslides triggered by the June 2013 extreme rainfall event in parts of Uttarakhand state, India. *Landslides*, **12**, 1, 135–146, doi: 10.1007/s10346-014-0540-7.
- Metwaly M., AlFouzan F., 2013: Application of 2-D geoelectrical resistivity tomography for subsurface cavity detection in the eastern part of Saudi Arabia. *Geosci. Front.*, **4**, 4, 469–476, doi: 10.1016/j.gsf.2012.12.005.
- NITI Aayog, 2018: Report of Working Group I: Inventory and Revival of Springs in the Himalayas for Water Security. Government of India, 52 p., accessed on April 7, 2022 at [https://lib.icimod.org/record/34336/files/NITI\\_Aayog\\_WGI.pdf](https://lib.icimod.org/record/34336/files/NITI_Aayog_WGI.pdf).
- Oldham T., 1883: The thermal springs of India. *Mem. Geol. Surv. India*, **19**, 99–140.
- Petley D., 2013: Reconstructing the events at Kedarnath using data, images and eyewitness reports. *The Landslides Blog*, 4 July 2013, accessed on April 7, 2022 at <http://blogs.agu.org/landslideblog>.
- Rai S. N., Thiagarajan S.; Kumar D., Dubey K. M., Rai P. K., Ramachandran A., Nithya B., 2013: Electrical resistivity tomography for groundwater exploration in a granitic terrain in NGRI campus. *Curr. Sci.*, **105**, 10, 1410–1418.
- Rana N., Singh S., Sundriyal Y. P., Juyal N., 2013: Recent and past floods in the Alaknanda valley: causes and consequences. *Curr. Sci.*, **105**, 9, 1209–1212.
- Rautela P., 2013: Lessons learnt from the Deluge of Kedarnath, Uttarakhand, India. *Asian J. Environ. Disaster Manag.*, **5**, 2, 43–51, doi: 10.3850/S1793924013002824.
- Rautela P., Sajwan K. S., Khanduri S., Ghildiyal S., Chanderkala, Rawat A., 2014: Geological investigations in Rudraprayag district with special reference to mass instability. *Disaster Management and Mitigation Centre, Govt. of Uttarakhand, Dehra Dun*, 117 p.
- Rawat P. K., 2013: *GIS modeling on mountain geodiversity and its hydrological responses in view of climate change*. LAP LAMBERT Academic Publishing, Saarbrücken, Germany, 188 p.

- Rawat P. K., 2014: GIS Development to monitor climate change and its geohydrological consequences on Nonmonsoon crop pattern in Lesser Himalaya. *Comput. Geosci.*, **70**, 80–95, doi: 10.1016/j.cageo.2014.04.010.
- Rawat P. K., Tiwari P. C., Pant C. C., 2012a: Geo-hydrological database modeling for integrated multiple hazard and risks assessment in Lesser Himalaya: A GIS based case study. *Nat. Hazards*, **62**, 3, 1233–1260, doi: 10.1007/s11069-012-0144-2.
- Rawat P. K., Pant C. C., Tiwari P. C., Pant P. D., Sharma A. K., 2012b: Spatial variability assessment of river-line floods and flash floods in Himalaya: A case study using GIS. *Disaster Prev. Manag.*, **21**, 2, 135–159, doi: 10.1108/09653561211219955.
- Sarkar T., Kannaujiya S., Taloor A. K., Champati Ray P. K., Chauhan P., 2020: Integrated study of GRACE data derived interannual groundwater storage variability over water stressed Indian regions. *Groundw. Sustain. Dev.*, **10**, 100376, doi: 10.1016/j.gsd.2020.100376.
- Sarkar T., Karunakalage A., Kannaujiya S., Chaganti C., 2022: Quantification of groundwater storage variation in Himalayan Peninsular River basins correlating with land deformation effects observed at different Indian cities. *Contrib. Geophys. Geod.*, **52**, 1, 1–56, doi: 10.31577/congeo.2022.52.1.1.
- Sasaki Y., 1992: Resolution of resistivity tomography inferred from numerical simulation. *Geophys. Prospect.*, **40**, 4, 453–463, doi: 10.1111/j.1365-2478.1992.tb00536.x.
- Schwartz F. W., Zhang H., 2003: *Fundamentals of Ground Water*. John Wiley & Sons Inc., New York, 592 p.
- Shanker R., Guha S. K., Seth N. N., Muthuraman K., Pitale U. L., Jangi B. L., Prakash G., Bandyopadhyay A. K., Sinha R. K., 1991: *Geothermal Atlas of India*. Geol. Surv. India, Kolkata, Spec. Publ. 19, 144 p.
- Singh S., Gautam P. K., Kumar P., Biswas A., Sarkar T., 2021: Delineating the characteristics of saline water intrusion in the coastal aquifers of Tamil Nadu, India by analysing the Dar-Zarrouk parameters. *Contrib. Geophys. Geod.*, **51**, 2, 141–163, doi: 10.31577/congeo.2021.51.2.3.
- Telford W. M., Geldart L. P., Sheriff R. E., 1990: *Applied geophysics*, 2nd edition. Cambridge University Press, 792 p.
- Uniyal A., 2013: Lessons from Kedarnath tragedy of Uttarakhand Himalaya, India. *Curr. Sci.*, **105**, 11, 1472–1474.
- Valdiya K. S., Bartarya S. K., 1991: Hydrogeological studies of springs in the catchment of Gaula River, Kumaun Lesser Himalaya, India. *Mt. Res. Dev.*, **11**, 3, 239–258, doi: 10.2307/3673618.
- Valdiya K. S., Paul S. K., Chandra T., Bhakuni S. S., Upadhyay R. C., 1999: Tectonic and lithological characterization of Himadri (Great Himalaya) between Kali and Yamuna rivers, Central Himalaya. *Himal. Geol.*, **20**, 2, 1–17.
- Velayudham J., Kannaujiya S., Sarkar T., Champati ray P. K., Taloor A. K., Singh Bisht M. P., Chawla S., Pal S. K., 2021: Comprehensive study on evaluation of Kaliasaur Landslide attributes in Garhwal Himalaya by the execution of geospatial, geotechnical and geophysical methods. *Quat. Sci. Adv.*, **3**, 100025, doi: 10.1016/j.qsa.2021.100025.

- Waring G. A., Blankenship R. R., Bentall R., 1965: Thermal Springs of the United States and Other Countries of the World – A Summary. U.S. Geological Survey, Professional Paper 492, Washington D.C.
- Wolke R., Schwetlick H., 1988: Iteratively reweighted least squares: algorithms, convergence analysis, and numerical comparisons. *SIAM J. Sci. Stat. Comput.*, **9**, 5, 907–921, doi: 10.1137/0909062.